iScience

CellPress

Article

The FDA-Approved Oral Drug Nitazoxanide Amplifies Host Antiviral Responses and Inhibits Ebola Virus

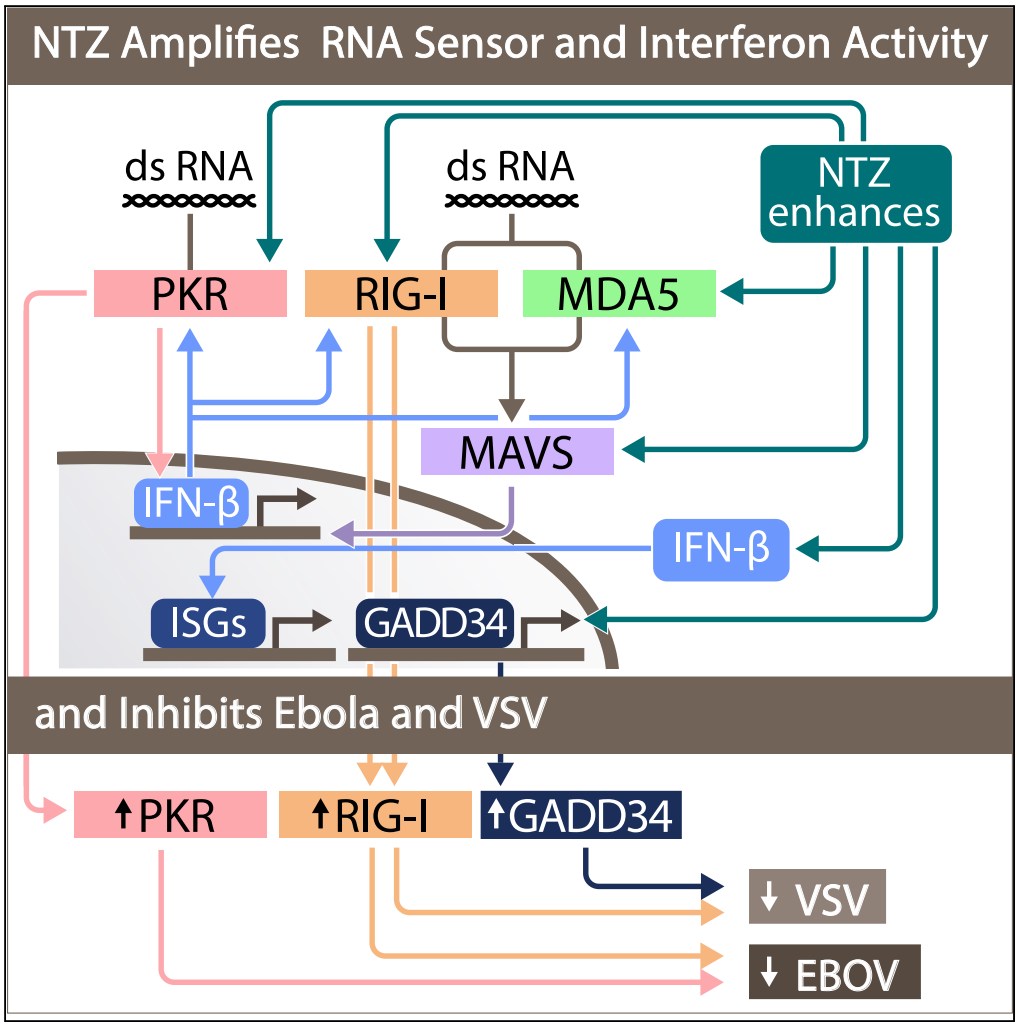

Luke D. Jasenosky, Cristhian Cadena, Chad E. Mire, ..., Thomas W. Geisbert, Sun Hur, Anne E. Goldfeld

anne.goldfeld@childrens.harvard.edu

HIGHLIGHTS

NTZ amplifies RNA sensor and type I interferon activities and induces GADD34 expression

NTZ inhibits infectious Ebola virus (EBOV) via RIG-I and PKR, but not GADD34

NTZ inhibits a second negative-strand RNA virus, VSV, via RIG-I and GADD34, but not PKR

NTZ holds promise as an oral therapy against EBOV

Jasenosky et al., iScience *19*, 1265–1276
September 27, 2019
https://doi.org/10.1016/j.isci.2019.07.003

iScience

CellPress

Article

The FDA-Approved Oral Drug Nitazoxanide Amplifies Host Antiviral Responses and Inhibits Ebola Virus

Luke D. Jasenosky,[1,7] Cristhian Cadena,[1] Chad E. Mire,[2] Viktoriya Borisevich,[2] Viraga Haridas,[1] Shahin Ranjbar,[1] Aya Nambu,[1] Sina Bavari,[3] Veronica Soloveva,[3,8] Supriya Sadukhan,[1] Gail H. Cassell,[4] Thomas W. Geisbert,[2] Sun Hur,[1] and Anne E. Goldfeld[1,5,6,9,*]

SUMMARY

Here, we show that the US Food and Drug Administration-approved oral drug nitazoxanide (NTZ) broadly amplifies the host innate immune response to viruses and inhibits Ebola virus (EBOV) replication. We find that NTZ enhances retinoic-acid-inducible protein I (RIG-I)-like-receptor, mitochondrial antiviral signaling protein, interferon regulatory factor 3, and interferon activities and induces transcription of the antiviral phosphatase GADD34. NTZ significantly inhibits EBOV replication in human cells through its effects on RIG-I and protein kinase R (PKR), suggesting that it counteracts EBOV VP35 protein's ability to block RIG-I and PKR sensing of EBOV. NTZ also inhibits a second negative-strand RNA virus, vesicular stomatitis virus (VSV), through RIG-I and GADD34, but not PKR, consistent with VSV's distinct host innate immune evasion mechanisms. Thus, NTZ counteracts varied virus-specific immune evasion strategies by generally enhancing the RNA sensing and interferon axis that is triggered by foreign cytoplasmic RNA exposure, and holds promise as an oral therapy against EBOV.

INTRODUCTION

Pathogenic viruses have evolved a diverse array of mechanisms to avoid or impair the host innate immune antiviral response (Unterholzner and Almine, 2019), particularly by evading those pathways that result in type I interferon (IFN) production and signaling (Garcia-Sastre, 2017). For example, Ebola virus (EBOV) relies on its structural protein VP35 to inhibit viral double-stranded RNA (dsRNA) sensing by retinoic-acid-inducible protein I (RIG-I) (Cardenas et al., 2006; Leung et al., 2010; Luthra et al., 2013) and the IFN-inducible double-stranded (ds)RNA sensor protein kinase R (PKR) (Feng et al., 2007; Schumann et al., 2009), thus avoiding the triggering and amplification of the host type I IFN response. The critical role played by VP35 in productive EBOV infection was underscored by the finding that mutations introduced into VP35 that disrupted its ability to sequester viral RNA intermediates, which did not affect its function in EBOV replication, resulted in increased type I IFN induction *in vitro* and severely attenuated viral growth *in vivo* in mice (Hartman et al., 2008) and guinea pigs (Prins et al., 2010). A host-directed therapy that could overcome this potent VP35-dependent EBOV immune evasion strategy would thus be particularly useful.

Nitazoxanide (NTZ) is an oral US Food and Drug Administration (FDA)-approved drug that has been used in millions of adults and children since 2004 with minimal adverse side effects for the treatment of *Giardia*- and *Cryptosporidium*-associated diarrhea, including in patients co-infected with HIV (Doumbo et al., 1997; Hussar, 2004; Rossignol et al., 1998). NTZ and its circulating metabolite tizoxanide (TIZ) have also been reported to inhibit a diverse array of viruses in tissue culture and in small animal models (Rossignol, 2014). In humans, NTZ reduces symptom duration of uncomplicated influenza (Haffizulla et al., 2014), viral gastroenteritis (Rossignol and El-Gohary, 2006), and rotaviral diarrhea (Rossignol et al., 2006). Several mechanisms have been proposed to contribute to NTZ's activity against specific viruses (Ashiru et al., 2014; La Frazia et al., 2013; Li et al., 2017; Piacentini et al., 2018; Rossignol et al., 2009b; Sekiba et al., 2018), including studies showing enhancement or induction of IFN-stimulated gene (ISG) expression by NTZ (Gekonge et al., 2015; Petersen et al., 2016; Trabattoni et al., 2016) and studies showing a weak association between NTZ and PKR activation (Ashiru et al., 2014; Elazar et al., 2009). However, no functional link between NTZ's antiviral activity and any specific ISG or with PKR has been demonstrated, and the molecular mechanisms underlying its broad-spectrum antiviral effects on host cells remain unknown.

[1]Program in Cellular and Molecular Medicine, Children's Hospital Boston, Harvard Medical School, Boston, MA 02115, USA

[2]Department of Microbiology and Immunology, University of Texas Medical Branch, Galveston, TX 77555, USA

[3]U.S. Army Medical Research Institute of Infectious Diseases, Fort Detrick, MD 21702, USA

[4]Department of Global Health and Social Medicine, Harvard Medical School, Boston, MA 02115, USA

[5]Infectious Disease Division, Department of Medicine, Brigham and Women's Hospital, Boston, MA 02115, USA

[6]Department of Immunology and Infectious Diseases, Harvard T.H. Chan School of Public Health, Boston, MA, USA

[7]Present address: Profectus Biosciences, Pearl River, NY 10965, USA

[8]Present address: Merck Research Laboratories, Boston, MA 02115, USA

[9]Lead Contact

*Correspondence: anne.goldfeld@childrens.harvard.edu

https://doi.org/10.1016/j.isci.2019.07.003

Here, we show that treatment of cells with NTZ results in broad amplification of the host innate immune response, including an increase in RIG-I-like receptor (RLR) activation in response to stimulation with cytoplasmic dsRNA, enhanced mitochondrial antiviral signaling protein (MAVS) and interferon regulatory factor 3 (IRF3) activities, and transcriptional induction of the antiviral phosphatase GADD34. Based on these data, we hypothesized that NTZ could limit or overcome EBOV's ability to evade detection by critical innate immune sensors following viral entry. At concentrations reflective of routine oral dosing for parasitic infections, NTZ significantly inhibits EBOV replication in A549 cells. Furthermore, using CRISPR/dead (d) Cas9-KRAB promoter targeting to ablate expression of individual host factors, we show that NTZ's inhibitory effect against EBOV relies on both RIG-I and PKR, indicating that NTZ can overcome EBOV VP35's ability to prevent viral detection by these cytoplasmic sensors. We also show that NTZ significantly inhibits a second negative-strand RNA virus, vesicular stomatitis virus (VSV), through a distinct mechanism involving both RIG-I and GADD34, but not PKR, consistent with the different innate immune evasion strategies employed by VSV when compared with EBOV. Thus, NTZ establishes a broad "antiviral" milieu that is rapidly amplified upon viral infection and is capable of counteracting varied virus-specific immune evasion strategies, such as those employed by EBOV and VSV.

With no effective and easily deployable oral drug to treat or prevent infection, EBOV caused over 10,000 deaths in the 2014–2016 west African EBOV epidemic (Shiwani et al., 2017) and has claimed over 1,700 lives to date (as of July 21, 2019) in the current outbreak in the Democratic Republic of the Congo (Claude et al., 2018; World Health Organization, 2019). Our demonstration that NTZ significantly inhibits EBOV replication *in vitro* suggests that NTZ could have a potential role in the treatment of acute EBOV disease, prevention of EBOV infection in exposed healthy individuals, and eradication of EBOV reservoirs that persist in immune-privileged sites of patients who have been cured of EBOV disease (Deen et al., 2017), and it provides impetus to test NTZ in animal models of EBOV infection to demonstrate *in vivo* efficacy.

RESULTS

To test whether NTZ enhances sensing by the RLR pathway, we overexpressed full-length RIG-I or melanoma differentiation-associated protein 5 (MDA5), the two major RLR proteins, in human embryonic kidney (HEK) 293T cells that were co-transfected with an IFN-β promoter-driven luciferase reporter plasmid (IFN-β LUC). We then examined whether NTZ augmented IFN-β promoter activity in the presence or absence of a viral nucleic acid analog, the synthetic dsRNA poly I:C. NTZ pretreatment enhanced poly I:C-stimulated IFN-β promoter activity in RIG-I- (Figure 1A, left) and in MDA5- (Figure 1A, right) overexpressing cells in a dose-dependent manner (Figure 1A). In the case of MDA5 overexpression, NTZ's effect on IFN-β reporter gene activity was evident even in the absence of poly I:C treatment (Figure 1A, right).

RIG-I and MDA5 differentially recognize distinct viral RNA signatures (Kato et al., 2006). RIG-I preferentially recognizes 5′ triphosphosphorylated short dsRNA structures typically generated by negative-strand RNA viruses, whereas MDA5 recognizes longer dsRNA structures (Kato et al., 2008; Schlee et al., 2009). To more precisely distinguish NTZ's effects on these RNA sensors, we next tested the effect of NTZ on a more specific RIG-I stimulus by using a short (42 bp) 5′ phosphorylated synthetic dsRNA (1AB) (Peisley et al., 2013). We found that IFN-β reporter activity was also significantly enhanced by NTZ in the RIG-I-overexpressing cells that were stimulated with 1AB (Figure 1B, left panel). Furthermore, endogenous IFN-β mRNA synthesis was significantly enhanced by NTZ pretreatment before 1AB stimulation of 293T cells (Figure 1B, right panel).

We next tested the ability of NTZ pretreatment to activate IFN-β reporter gene activity in HEK293T cells co-transfected with a plasmid overexpressing MAVS, the adaptor protein through which RIG-I and MDA5 signal (Kawai et al., 2005; Meylan et al., 2005; Seth et al., 2005; Xu et al., 2005). IFN-β LUC activity was strongly enhanced by NTZ in MAVS-overexpressing cells even in the absence of any other cellular stimulation, reaching a >4-fold increase at a concentration of 10 μM NTZ (Figure 1C).

It has been reported that in addition to preventing IRF3 phosphorylation and activation by blocking RIG-I viral RNA sensing, EBOV VP35 also prevents IRF3 phosphorylation by directly blocking the access of the kinases IKKε and TBK-1 to unphosphorylated IRF3 (Prins et al., 2009). To determine if NTZ can directly augment IRF3's activity, we next transfected HEK293T cells with a plasmid encoding phosphomimetic IRF3, which is able to drive IFN-β mRNA expression in the absence of proximal components of the RLR signaling pathway (Lin et al., 1998). As shown in Figure 1D, NTZ enhanced IRF3-induced IFN-β reporter

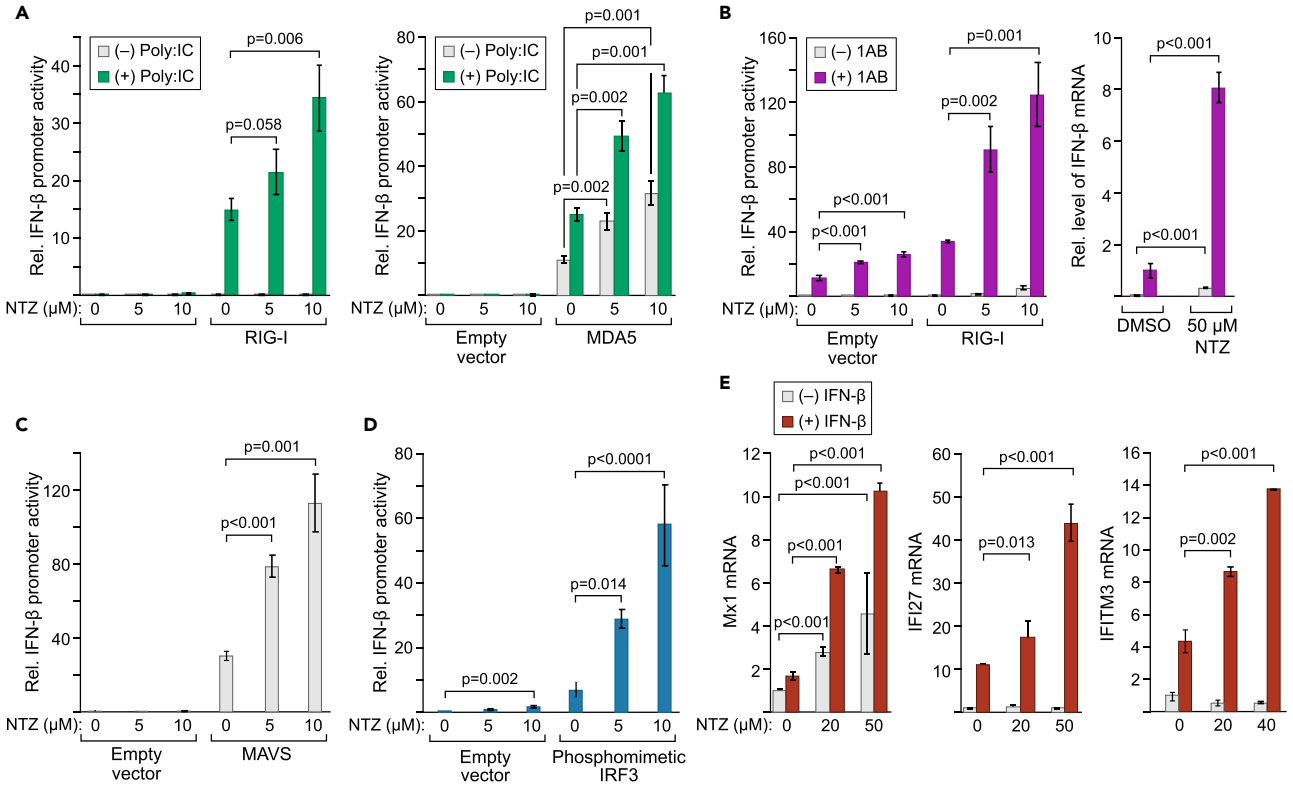

Figure 1. NTZ Broadly Enhances the IFN Pathway

(A) IFN-β reporter activity in HEK293T cells co-transfected with RIG-I (left panel) or MDA5 (right panel) expression vectors or empty vector control with increasing amounts of NTZ in the presence and absence of poly I:C. Values were normalized against IFN-β reporter activity with empty vector in the absence of NTZ and poly I:C. Error bars represent standard deviations.

(B) IFN-β reporter activity in HEK293T cells co-transfected with a RIG-I expression vector or empty vector control with increasing amount of NTZ in the presence and absence of 42bp 5′ppp dsRNA (1AB) (left panel). Values were normalized against the IFN-β reporter activity with empty vector in the absence of NTZ and 1AB. Relative expression of IFN-β mRNA in HEK293T cells stimulated with 1AB or mock in the presence or absence of NTZ (right panel). Values were calculated relative to the housekeeping gene GAPDH and normalized against mock 1AB-transfected HEK293T cells without NTZ (DMSO). Error bars represent standard deviations.

(C) IFN-β reporter activity in HEK293T cells co-transfected with MAVS or empty vector control with increasing amounts of NTZ. Values were normalized against the reporter activity with empty vector in the absence of NTZ. Error bars represent standard deviations.

(D) IFN-β reporter activity in HEK293T cells co-transfected with different concentrations of a phosphomimetic IRF3 (IRF3-5D) or empty vector control with increasing amount of NTZ. Values were normalized against the reporter activity with empty vector in the absence of NTZ. Error bars represent standard deviations.

(E) Relative expression of Mx1, IFI27, and IFITM3 mRNA in HEK293T cells treated with human recombinant IFN-β and increasing concentrations of NTZ. Values were calculated relative to the housekeeping gene GAPDH and normalized against no IFN-β treatment in the absence of NTZ. Error bars represent standard deviations.

activity in a dose-dependent manner. Furthermore, we also found that NTZ enhanced type I IFN-induced transcription of the ISGs Mx1, IFI27, and IFITM3 (Figure 1E). Thus, NTZ broadly enhances signaling downstream of the RLR and IFN-β signaling pathways in addition to acting as an agonist for viral RNA sensors acting at the proximal part of the pathway in the cytoplasm.

Physiological NTZ Concentrations Strongly Restrict EBOV Replication

Our data that NTZ broadly enhances antiviral sensing via the cytoplasmic RLR pathway and amplifies type I IFN-induced gene expression, including IFITM3 gene synthesis, which has previously been shown to inhibit EBOV infection (Huang et al., 2011), led us to speculate that NTZ may overcome EBOV's capacity to evade host RNA sensing and to skirt triggering of the type I IFN response (Basler et al., 2000, 2003; Cardenas et al., 2006; Hartman et al., 2008; Leung et al., 2010; Luthra et al., 2013), thus favoring host control of the virus. To test this hypothesis, we examined the ability of NTZ to inhibit infectious EBOV growth in human pulmonary epithelial A549 cells *in vitro* under biosafety level 4 conditions using an isolate of infectious EBOV from the

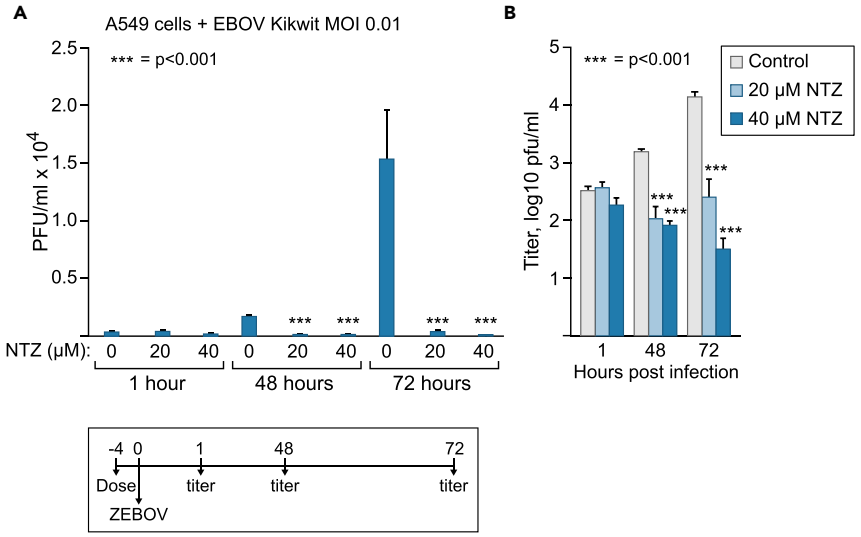

Figure 2. NTZ Inhibits EBOV Infection/Replication in A549 Cells

A549 cells were mock-treated or treated with 20 or 40 μM NTZ for 4 h and infected with EBOV-Kikwit at MOI of 0.01 in the presence of the cellular supernatants from the NTZ-pretreated cells. Supernatants were harvested at 1, 48, or 72 h post-infection, clarified, and EBOV plaque-forming unit (PFU) was calculated by plaque assay. Results shown as PFU/mL (A) and $\log_{10}$ PFU/mL (B). ***$p < 0.001$. When NTZ was added 24 h before Ebola infection it similarly inhibited viral growth.

original 1995 outbreak in the Democratic Republic of the Congo (Kikwit). Cells were pretreated with 0, 20, or 40 μM NTZ, which is not toxic to A549 cells (see Figure 3A), for 4 h, and were then infected with EBOV at an MOI of 0.01. As shown in Figure 2, in vehicle-only treated cells, EBOV growth increased by over 1.5 log units by 72 h post-infection. By contrast, over the same time frame, EBOV growth was completely inhibited in cells treated with 20 or 40 μM of NTZ ($p < 0.001$), dropping 2.5 log units from the initial inoculum titer in the cells treated with 40 μM NTZ ($p < 0.001$). We note that 20 and 40 μM are concentrations of NTZ that are either well below or equivalent to peak plasma levels (~39 μM) of its active metabolite TIZ that are observed in humans who have ingested 500 mg of NTZ twice a day in a typical oral regimen for cryptosporidial diarrhea (Romark, 2017).

NTZ Inhibits VSV Replication through RIG-I but Not PKR

To begin to characterize the mechanisms involved in NTZ's antiviral activity, we next tested NTZ's effect on a second RNA virus, the rhabdovirus VSV, which, like EBOV, is a member of the order Mononegavirales, and which also allowed testing under biosafety level 2 conditions. NTZ pretreatment of A549 cells for 4 h inhibited the growth of a firefly luciferase-expressing VSV (VSV-Luc) reporter virus (Cureton et al., 2012) in A549 cells, with greater than 99% inhibition of VSV-Luc achieved at an NTZ concentration of 12 μM and >99.9% inhibition obtained at 18 μM (Figure 3A, left).

Given the importance of both RIG-I and PKR in EBOV's evasion of the host antiviral response (Cardenas et al., 2006; Feng et al., 2007; Leung et al., 2010; Luthra et al., 2013; Schumann et al., 2009), and reports that NTZ can weakly induce auto-phosphorylation of PKR (Ashiru et al., 2014; Elazar et al., 2009), we next sought to determine the role of these molecules in NTZ's antiviral activity using the VSV model system. Because traditional short hairpin RNA (shRNA)-based methods of gene knockdown, including in A549 cells, are associated with both non-specific type I IFN induction by the shRNA itself, and reduced shRNA activity in response to type I IFN stimulation (Machitani et al., 2017), we chose to knockdown RIG-I or PKR expression in A549 cells by targeting dead(d)Cas9-KRAB to their genes' promoters (see Transparent Methods and Figure S1 for gRNA target sequences and Figure 3B for protein knockdown efficiency). RIG-I depletion (Figure 3C, left panel) led to significantly increased VSV-Luc growth (Figure 3C, right panel, see 0 μM NTZ data point) and to a strong reduction in VSV-Luc's sensitivity to NTZ (50% inhibition at 4.8 μM NTZ in CRISPR-Ctrl A549 cells versus 8.0 μM NTZ in CRISPR-RIG-I A549 cells) (Figure 3C, right panel). Depletion of PKR (Figure 3D, left panel) also resulted in significantly increased VSV-Luc growth (Figure 3D, right panel, 0 μM NTZ data point). However, NTZ's ability to block VSV replication was not impaired in PKR-depleted cells

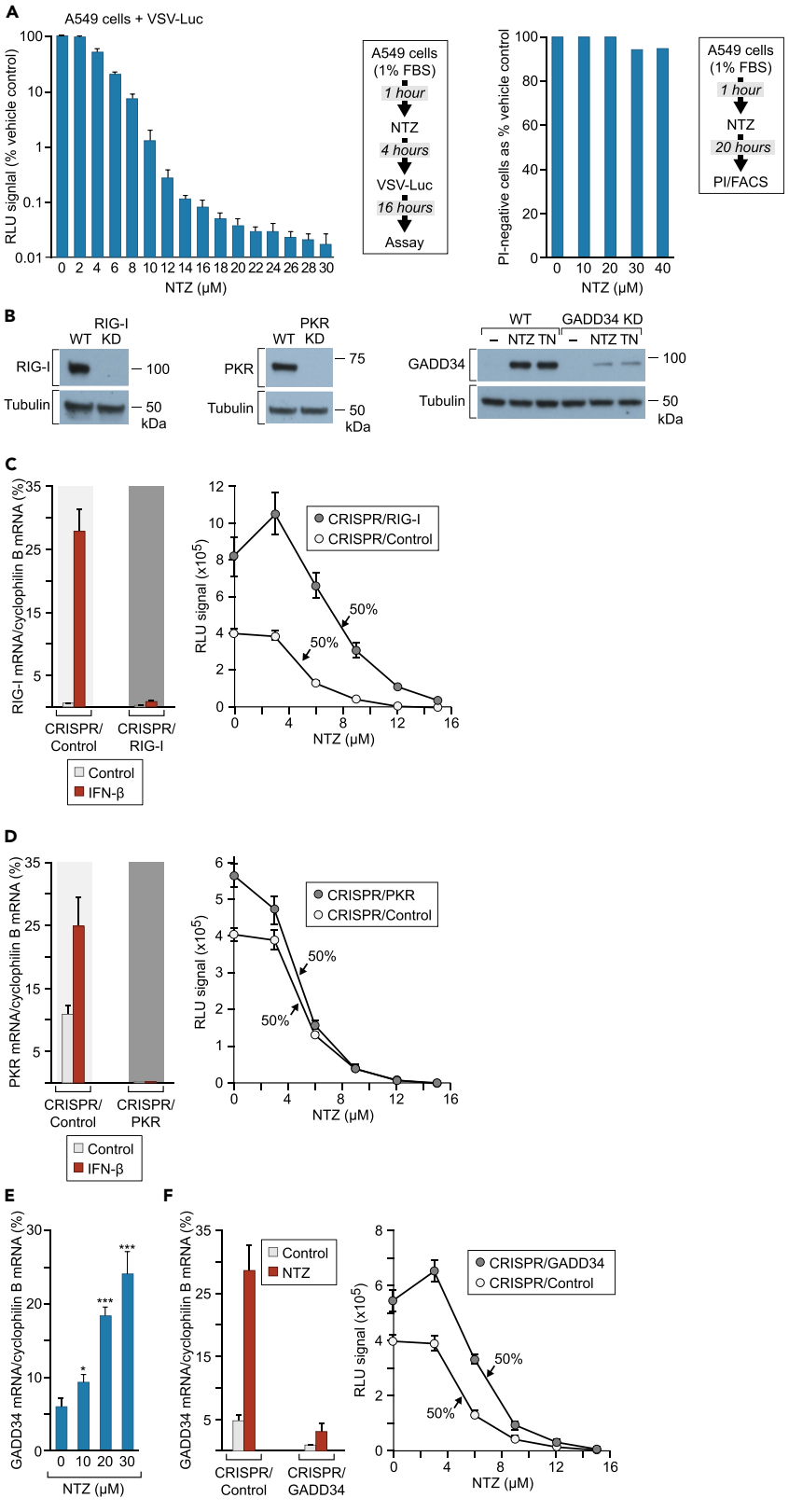
A
A549 cells + VSV-Luc
RLU signal (% vehicle control)
NTZ (μM)
A549 cells
(1% FBS)
1 hour
NTZ
4 hours
VSV-Luc
16 hours
Assay
PI-negative cells as % vehicle control
NTZ (μM)
A549 cells
(1% FBS)
1 hour
NTZ
20 hours
PI/FACS
B
RIG-I
WT KD
RIG-I
Tubulin
100
50
kDa
PKR
WT KD
PKR
Tubulin
75
50
kDa
WT GADD34 KD
NTZ TN NTZ TN
GADD34
Tubulin
100
50
kDa
C
RIG-I mRNA/cyclophilin B mRNA (%)
CRISPR/
Control
CRISPR/
RIG-I
Control
IFN-β
RLU signal (x10^5)
CRISPR/RIG-I
CRISPR/Control
50%
50%
NTZ (μM)
D
PKR mRNA/cyclophilin B mRNA (%)
CRISPR/
Control
CRISPR/
PKR
Control
IFN-β
RLU signal (x10^5)
CRISPR/PKR
CRISPR/Control
50%
50%
NTZ (μM)
E
GADD34 mRNA/cyclophilin B mRNA (%)
NTZ (μM)
F
GADD34 mRNA/cyclophilin B mRNA (%)
Control
NTZ
CRISPR/
Control
CRISPR/
GADD34
RLU signal (x10^5)
CRISPR/GADD34
CRISPR/Control
50%
50%
NTZ (μM)

Figure 3. NTZ Strongly Inhibits VSV Infection/Replication in A549 Cells: Depletion of RIG-I and GADD34, but Not PKR, Impairs Anti-VSV Activity of NTZ

(A) Left panel: A549 cells were treated with NTZ at the indicated concentrations for 4 h and were then infected with a VSV firefly luciferase reporter (Cureton et al., 2012). After 16 h, cells were harvested and firefly luciferase activity was measured by luminescence assay. Means and standard deviations from three independent experiments performed in duplicate are shown. Right panel: A549 cells were treated with vehicle or NTZ at the indicated concentrations for 18 h. Cells were harvested, exposed to 1 μM propidium iodide for 5 min, and subjected to flow cytometry.

(B) Protein expression levels were efficiently knocked down in A549 cells by CRISPR/dCas9-KRAB in combination with guide RNA (gRNA) targeting the promoters of the RIG-I, PKR, or GADD34 genes, respectively. Protein expression levels of RIG-I, PKR, and GADD34 were evaluated by western blot analysis. For GADD34, cells were stimulated by vehicle control DMSO (—) at 0.1%, tunicamycin (TN) at 10 μg/mL or nitazoxanide (NTZ) at 25 μM for 8 h.

(C) Left panel: lentiviral targeting of dCas9-KRAB to the RIG-I gene promoter in A549 cells inhibits RIG-I gene expression in both the absence and presence of IFN-β stimulation. Right panel: CRISPR-control or CRISPR-RIG-I A549 cells were seeded at equal density, treated with NTZ at the indicated concentrations for 4 h, infected with VSV-Luc for 16 h, and firefly luciferase activity was quantitated. Means and standard errors are shown from three independent experiments performed in duplicate. NTZ inhibitory activity is presented as firefly luciferase signal as a percentage of vehicle (DMSO) control. Forward and reverse qPCR primer pairs: Cyclophilin B, 5′-AGAAGAAGGGGCCCAAAGT-3′, 5′-AAAGATCACCCGGCCTACAT-3′; RIG-I, 5′-GAAGACCCTGGACCCTACCTA-3′, 5′-CCATTGGGCCCTTGTTGTTT-3′.

(D) Left panel: lentiviral targeting of dCas9-KRAB to the PKR gene promoter in A549 cells potently inhibits PKR gene expression in both the absence and presence of IFN-β stimulation. Right panel: CRISPR-control or CRISPR-PKR A549 cells were seeded at equal density, treated with NTZ at the indicated concentrations for 4 h, infected with VSV-Luc for 16 h, and firefly luciferase activity was quantitated. Means and standard errors are shown from three independent experiments performed in duplicate. NTZ inhibitory activity is presented as firefly luciferase signal as a percentage of vehicle (DMSO) control. Forward and reverse qPCR primer pairs: Cyclophilin B as in (B); PKR, 5′-TTTGGACAAAGCTTCCAACC-3′, 5′-CTACTCCCTGCTTCTGACGG-3′.

(E) A549 cells were mock-treated or treated with 10, 20, or 40 μM NTZ for 4 h and GADD34 transcript levels were measured. We note that we tested a range of time points between 1 and 8 h after 40 μM NTZ stimulation of A549 cells and found that GADD34 mRNA levels peaked between 4 and 8 h (data not shown). GADD34 transcript levels are expressed as a percentage of the housekeeping gene cyclophilin B. Mean and SD of three independent experiments are shown. *$p < 0.05$, ***$p < 0.001$. Forward and reverse qPCR primer pairs: Cyclophilin B as in (B); GADD34, 5′-GGTGCCAACCCAGTGATGAA-3′, 5′-TTCAGGAAGGCACTTGGTGG-3′.

(F) Left panel: lentiviral targeting of dCas9-KRAB to the GADD34 gene promoter in A549 cells strongly inhibits GADD34 gene expression in both the absence and presence of NTZ stimulation. Right panel: CRISPR-control or CRISPR-GADD34 A549 cells were seeded at equal density, treated with NTZ at the indicated concentrations for 4 h, infected with VSV-Luc for 16 h, and firefly luciferase activity was quantitated. Means and standard errors are shown from three independent experiments performed in duplicate. NTZ inhibitory activity is presented as firefly luciferase signal as a percentage of vehicle (DMSO) control. Forward and reverse qPCR primer pairs are described in (D).

at any NTZ concentration tested (50% inhibition with 4.8 μM NTZ in CRISPR-Ctrl A549 cells versus 4.7 μM NTZ in CRISPR-PKR A549 cells) (Figure 3D, right panel), indicating that NTZ's suppression of VSV replication is not dependent on PKR.

NTZ Inhibition of VSV Growth Depends in Part on GADD34

The phosphatase GADD34 selectively promotes IFN-β translation in the context of host global translational shutdown following PKR-dependent eIF2α phosphorylation or stress pathway activation (Dalet et al., 2017). NTZ has previously been shown to induce low levels of endoplasmic reticulum stress (Ashiru et al., 2014) and to promote the translation of the transcription factor ATF4 (Elazar et al., 2009), which during translational inhibition is a transcriptional activator of GADD34 gene expression (Ma and Hendershot, 2003). We thus investigated whether NTZ affected GADD34 expression. We treated A549 cells with increasing concentrations of NTZ for 4 h and measured GADD34 mRNA levels. NTZ strongly induced GADD34 mRNA synthesis in an NTZ concentration-dependent manner (Figure 3E). We note that maximal GADD34 transcription was detected between 4 and 8 h post-NTZ stimulation of A549 cells (not shown).

To investigate whether GADD34 participates in NTZ's inhibitory effect on VSV, we knocked down GADD34 in A549 cells using the CRISPR/dCas9-KRAB strategy described above (see Transparent Methods and Figures S1 and 3B) and infected these GADD34-depleted A549 cells (Figure 3F, left panel) with the VSV-Luc reporter virus. GADD34 depletion resulted in a significant increase in VSV infection/growth (Figure 3F, right panel, 0 μM NTZ data point), similar to previously reported findings with VSV and GADD34$^{-/-}$ mouse embryonic fibroblasts (Minami et al., 2007). Furthermore, GADD34 depletion reduced VSV sensitivity to NTZ (50% inhibition at 4.8 μM NTZ in CRISPR-Ctrl A549 cells versus at 6.9 μM NTZ in GADD34-KD A549 cells)

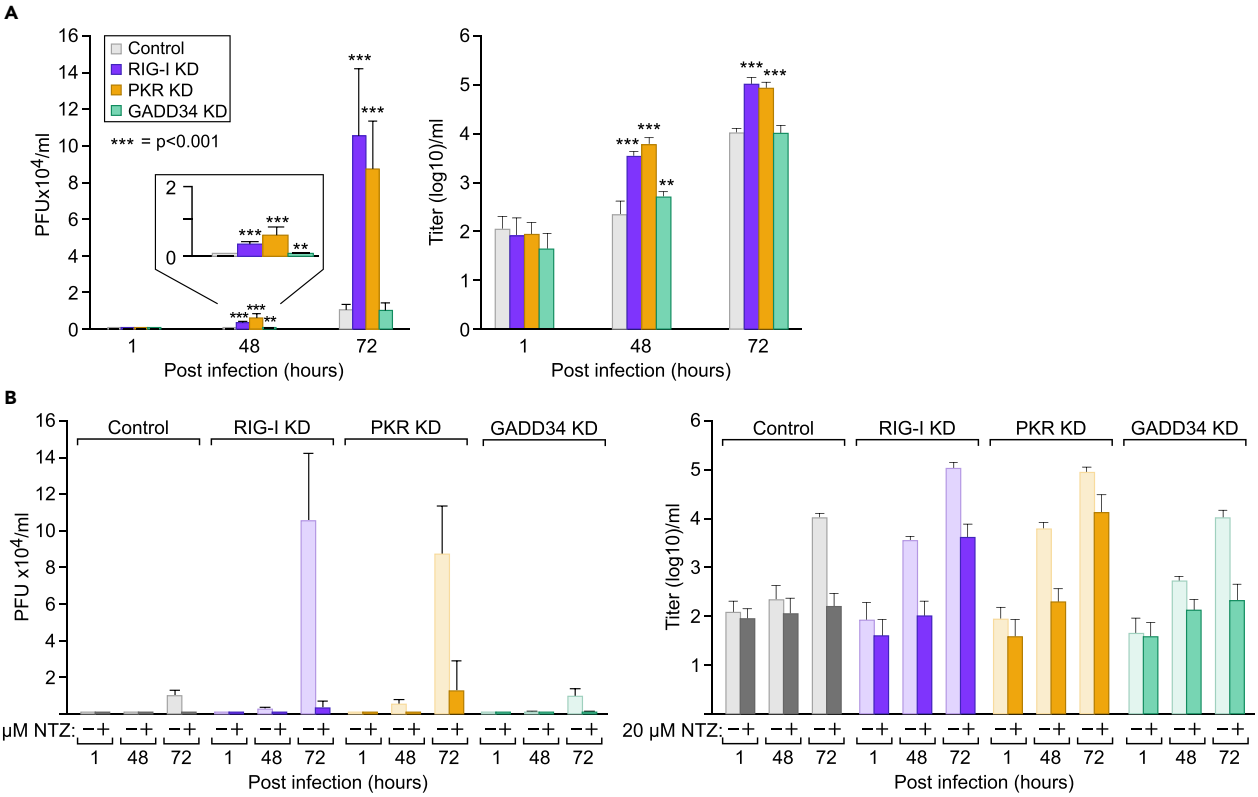

Figure 4. NTZ Requires PKR and RIG-I, but Not GADD34, for Full Inhibition of EBOV Replication in A549 Cells

(A) Knockdown of RIG-I and PKR in A549 cells augments EBOV replication, whereas knockdown of GADD34 has a more modest effect on EBOV growth. Cells were mock-treated or treated with 20 μM NTZ for 4 h and infected with EBOV at MOI of 0.01 in the presence of pretreatment NTZ supernatants. Supernatants were harvested at 1, 48, or 72 h, clarified, and EBOV plaque-forming unit (PFU) was calculated by plaque assay. Titers are displayed on linear (left) and log (right) scales for clarity. **$p < 0.01$, ***$p < 0.001$.

(B) Compared with control A549 cells, NTZ inhibition of EBOV replication is impaired in RIG-I-KD and PKR-KD A549 cells but is not affected by GADD34 knockdown. Cells were mock-treated or treated with 20 μM NTZ for 4 h and infected with EBOV at MOI of 0.01 in the presence of pretreatment NTZ supernatants. Supernatants were harvested at 1, 48, or 72 h, clarified, and EBOV PFU was calculated by plaque assay. Titers are displayed on linear (left) and log (right) scales for clarity.

(Figure 3F, right panel), indicating that NTZ's anti-VSV activity also depends on its ability to induce the expression of GADD34 in addition to its enhancement of RIG-I function. Taken together, although RIG-I, PKR, and GADD34, play a role in host inhibition of VSV, only RIG-I and GADD34, and not PKR, are involved in NTZ-mediated repression of this virus.

NTZ Suppresses EBOV Replication through RIG-I and PKR

We next analyzed EBOV replication in the CRISPR/dCas9-RIG-I-KD, PKR-KD, and GADD34-KD A549 cells under biosafety level 4 conditions to determine the individual roles of these antiviral proteins in restricting EBOV growth. Both RIG-I and PKR depletion led to significantly increased EBOV Kikwit replication (Figure 4A), with an increase of greater than a log unit by 72 h post-infection when compared with control cells (Figure 4A, right). This experiment demonstrates the importance of both factors in host control of EBOV infection. By contrast, although GADD34 depletion resulted in higher EBOV titers at 48 h, it did not impact EBOV growth by 72 h post-infection (Figure 4A, right). Thus, unlike what we found with VSV, GADD34 plays a limited role in restricting EBOV growth in A549 cells.

To determine if RIG-I, PKR, or GADD34 were targets of NTZ and required for its inhibitory effects upon EBOV, we next pretreated the CRISPR/dCas9-KRAB nonspecific control cells and the CRISPR/dCas9-RIG-I-KD, PKR-KD, or GADD34-KD A549 cell lines with 0 or 20 μM NTZ for 4 h and then infected with EBOV Kikwit at an MOI of 0.01. As shown in Figure 4B (left), there was a 10.5-fold reduction (>1 log change)

in NTZ's anti-EBOV activity in CRISPR/PKR-KD A549 cells by 72 h post-infection when compared with the CRISPR/Control A549 cells, indicating that PKR activity plays a critical role in NTZ's efficacy against EBOV. RIG-I depletion also resulted in an appreciable, although lesser, reduction in EBOV sensitivity to NTZ (2.7-fold) by 72 h post-infection (Figure 4B). By contrast, GADD34 depletion had little effect on NTZ's ability to inhibit EBOV growth (Figure 4B).

DISCUSSION

Here, we have shown that the FDA-approved small molecule drug NTZ broadly amplifies cytoplasmic RNA sensing and type I IFN pathways and strongly inhibits replication of EBOV and VSV. Our data indicate that NTZ's amplification of RIG-I and PKR activities overcomes EBOV VP35's ability to prevent the triggering of these critical host antiviral factors. By contrast, in the case of VSV, NTZ-mediated amplification of RIG-I signaling and induction of GADD34 expression, both contribute to the drug's anti-VSV activity. Thus, the wide array of innate immune activities that NTZ amplifies provides cells with the capacity to resist productive infection by diverse viruses like EBOV and VSV that engage distinct host evasion mechanisms.

VP35 blocks RIG-I-driven type I IFN production and PKR activation by both sequestering dsRNA intermediates and binding to the PKR/RIG-I activator PACT (Bale et al., 2013; Cardenas et al., 2006; Feng et al., 2007; Leung et al., 2010; Luthra et al., 2013; Schumann et al., 2009). Furthermore, mutations in the dsRNA-binding pocket of EBOV VP35 were found to increase type I IFN induction *in vitro* and severely attenuate viral growth *in vivo* (Hartman et al., 2008; Prins et al., 2010). However, the relative importance of individual dsRNA-triggered cytoplasmic sensors for control of EBOV replication has not been clearly delineated. Our data here show that dCas9-KRAB-mediated knockdown of either RIG-I or PKR in A549 cells leads to a significant increase in EBOV replication (~1 log) after 72 h, directly demonstrating that both these host molecules contribute to control of EBOV growth. The fact that a wild-type clinical EBOV isolate with an intact VP35 as part of its genome is still susceptible to the effects of RIG-I and PKR underscores the critical roles played by both these factors in host control of EBOV. Furthermore, our data showing that NTZ's efficacy against EBOV is reduced when host cell expression of either PKR or RIG-I is ablated, indicates that the ability of NTZ to increase the activity of PKR and RIG-I at an early stage of EBOV infection, can tip the balance in favor of the host by blunting VP35's ability to suppress the innate immune response.

NTZ also suppressed VSV replication, and its antiviral efficacy was markedly reduced upon depletion of RIG-I in A549 cells. However, unlike what we observed for EBOV, knockdown of PKR had no effect on NTZ inhibition of VSV. Furthermore, in the absence of NTZ, we found that knockdown of PKR resulted in a significant but milder increase in VSV growth relative to the robust increase in EBOV replication we observed when PKR expression was ablated. We note that the VSV matrix protein blocks host cell type I IFN responses independently of PKR by inhibiting global mRNA synthesis and nuclear export, as well as by inhibiting global host protein synthesis (Ahmed et al., 2003; Black and Lyles, 1992; Connor and Lyles, 2005; Ferran and Lucas-Lenard, 1997; von Kobbe et al., 2000). The VSV matrix protein shuts down host cell translation primarily by inducing dephosphorylation of the eIF4F initiation complex component eIF4E (Connor and Lyles, 2002, 2005). However, eIF2α also becomes phosphorylated at later stages of VSV infection, leading to additional negative effects on host protein synthesis, including on type I IFN production, as well as on viral protein synthesis (Connor and Lyles, 2005). Here, we have shown that NTZ induces transcription and translation of GADD34, which is a phosphatase that reverses eIF2α phosphorylation (Novoa et al., 2001), and has been shown to be critical for restoring translation of IFN-β and other selected cytokines in virus-infected cells (Clavarino et al., 2012a, 2012b; Dalet et al., 2017). Given that GADD34 depletion reduces NTZ activity against VSV, our data suggest that NTZ induction of GADD34 further amplifies NTZ-augmented RIG-I signaling, providing cells with the capacity to mount an innate immune response that is sufficient to overcome VSV matrix protein inhibitory effects upon protein synthesis.

Our data also show that the activities of factors downstream of the RLRs are amplified by NTZ. Both overexpressed MAVS and constitutively phosphorylated IRF3 activities were amplified in response to NTZ stimulation, resulting in increased type I IFN promoter activity. NTZ also enhanced type I IFN-induced mRNA synthesis of ISGs Mx1, IFI27, and IFITM3. IFITM3 is a critical restriction factor for both EBOV (Huang et al., 2011) and VSV (Huang et al., 2011; Weidner et al., 2010), and Mx1 has been shown to inhibit VSV infection (Staeheli and Pavlovic, 1991). Thus, NTZ's ability to amplify both proximal and distal aspects of the viral RNA sensing and type I IFN pathways allows for a broad and effective antiviral response to develop in cells that are immediate viral targets and in neighboring cells yet to be infected.

Although three previous reports have suggested that ISGs induced by NTZ or its metabolite TIZ play an antiviral role, a direct functional impact of NTZ or TIZ upon any of these genes with respect to inhibition of viral growth, has not been shown. For example, one report described increased average expression of a panel of 26 ISGs in peripheral blood mononuclear cells (PBMCs) treated with a very low concentration (0.1 μM) of NTZ for an unspecified time, with no functional demonstration of how any of these individual ISGs affected replication of a virus in NTZ-treated cells (Petersen et al., 2016). Another article reported that treatment of human monocyte-derived macrophages (MDM) with NTZ for 48 h induced the expression of the ISGs tetherin and APOBEC3A/G, and although the authors associated this with NTZ inhibition of HIV in MDMs, no functional demonstration was provided showing that these molecules played any role in NTZ's anti-HIV activity (Gekonge et al., 2015). A third study reported that TIZ treatment of human PBMCs for 7 days induced a set of 14 IFNs and ISGs approximately 2-fold when compared with untreated PBMCs, with a slightly greater increase, on average, observed in the context of HIV infection (including Mx1, 1.8- to 2.9-fold respectively); however, again, no functional links between the ISGs identified and NTZ inhibition of HIV replication were made, and no mechanism for this response was investigated (Trabattoni et al., 2016). In contrast to the above studies, through both biochemical and gene knockdown approaches we have demonstrated that NTZ treatment results in broad amplification of RLR pathway components that are primary drivers of type I IFN production and ISG induction and amplifies type I IFN signaling. Furthermore, we have functionally linked RIG-I and PKR to NTZ's antiviral activity against EBOV, and functionally linked RIG-I and GADD34 to NTZ's activity against VSV using CRISPR/dCas9-KRAB-mediated knockdown of these molecules in host cells.

It has also been previously reported that NTZ induces phosphorylation of PKR in different cell lines. However, weak NTZ-induced PKR phosphorylation was only observed in one study after 72 h of 0.5 or 5 μM NTZ exposure in human hepatoma cells harboring an hepatitis C virus (HCV) replicon (Elazar et al., 2009), and after 24 h in a bovine kidney cell line with 25 μM, but not 10 μM, NTZ in another study (Ashiru et al., 2014). Furthermore, in both reports, no direct functional link between putative PKR phosphorylation by NTZ and its antiviral activity was demonstrated, thus leaving unverified the functional importance of PKR, or its phosphorylation status, for NTZ's ability to suppress replication of PKR-sensitive viruses. By contrast, our demonstration that the effect of NTZ on EBOV growth is markedly impaired in cells where PKR expression has been ablated directly links NTZ pretreatment for 4 h before EBOV infection to PKR restriction of EBOV growth.

Synthetic RLR agonists for the treatment of viruses have generated much interest (Yong and Luo, 2018). However, because RLRs are expressed in most human tissues and the inflammatory response to their induction is highly variable person to person, there is concern that therapeutic approaches employing RNA agonists will be associated with unacceptable inflammatory side effects (Elion and Cook, 2018). Intriguingly, NTZ has been used extensively with an excellent safety profile in adults and children for treatment of parasitic infections (Doumbo et al., 1997; Hussar, 2004; Rossignol et al., 1998), and for viral diseases such as HCV (Rossignol et al., 2008, 2009a) and influenza (Haffizulla et al., 2014). Notably, our findings indicate that NTZ modulate the innate immune response after a pathogen has entered a susceptible target cell, when amplification of natural immune control of viral infection is needed. In the case of viruses like EBOV that employ immune evasion mechanisms to avoid triggering the innate immune response, such a therapeutic profile is attractive. Although identification of NTZ's upstream target is outside the scope of this article, we anticipate that these studies, which are underway, will be of great value in unraveling host pathways that lead to cell-intrinsic control of Ebola.

Finally, the studies presented here suggest that after validation in an *in vivo* animal model, NTZ could be potentially useful in EBOV disease as monotherapy or as an adjuvant therapy with agents that specifically target EBOV components. Furthermore, NTZ may also prove valuable in strategies to prevent EBOV infection or to eradicate EBOV reservoirs that persist in patients who have survived EBOV disease.

Limitations of the Study

Although NTZ is FDA approved for the treatment of cryptosporidial diarrhea and is a well-tolerated medication, a limitation of the data presented here regarding NTZ's inhibition of EBOV is that it is based on *in vitro* studies and we have not yet established NTZ's efficacy against EBOV in an *in vivo* animal model. Furthermore, the detailed investigation of NTZ's upstream target in the regulation of the immune

responses described here is outside the scope of this article and will be the subject of future studies, as will *in vivo* testing of NTZ against EBOV.

METHODS

All methods can be found in the accompanying Transparent Methods supplemental file.

SUPPLEMENTAL INFORMATION

Supplemental Information can be found online at https://doi.org/10.1016/j.isci.2019.07.003.

ACKNOWLEDGMENTS

We are indebted to Wallis Annenberg and John Moores for their critical support making this study possible. This work was funded by a grant from the Annenberg Foundation, a gift from John Moores, and grants from the NIH (AI125075) and the Ragon Institute to A.E.G, and from the NIH to S.H. (AI106912 & AI111784), and to T.W.G. (U19AI109711). The funders had no role in study design, data collection and analysis, decision to publish, or preparation of the manuscript. We also thank James LeDuc and James Hodge for their advice, Martin Dorf for the gift of the VSV luciferase reporter virus, Renate Hellmiss for the artwork, and James Falvo for critical reading of the manuscript.

AUTHOR CONTRIBUTIONS

L.D.J. and A.E.G. planned the study. L.D.J., C.E.M., S.H., S.B., T.W.G., and A.E.G. designed the experiments. L.D.J., C.C., V.H., S.R., S.S., and A.N. performed experiments under BSL-2 conditions. C.E.M., V.B., and V.S. performed experiments under BSL-4 conditions. L.D.J. and A.E.G. wrote the paper.

DECLARATION OF INTERESTS

A.E.G.'s lab received a general laboratory gift from Romark Inc., which had no role in the conceptualization, design, data collection, analysis, decision to publish, or preparation of the manuscript. L.D.J., S.R., V.H., and A.E.G. are co-inventors on the patent "Treatment of Infectious Diseases", US15/546390 Jan 26 2015. The authors claim no other competing interests.

Received: March 25, 2019
Revised: June 3, 2019
Accepted: June 28, 2019
Published: August 8, 2019

REFERENCES

Ahmed, M., McKenzie, M.O., Puckett, S., Hojnacki, M., Poliquin, L., and Lyles, D.S. (2003). Ability of the matrix protein of vesicular stomatitis virus to suppress beta interferon gene expression is genetically correlated with the inhibition of host RNA and protein synthesis. J. Virol. *77*, 4646–4657.

Ashiru, O., Howe, J.D., and Butters, T.D. (2014). Nitazoxanide, an antiviral thiazolide, depletes ATP-sensitive intracellular Ca(2+) stores. Virology *462-463*, 135–148.

Bale, S., Julien, J.P., Bornholdt, Z.A., Krois, A.S., Wilson, I.A., and Saphire, E.O. (2013). Ebolavirus VP35 coats the backbone of double-stranded RNA for interferon antagonism. J. Virol. *87*, 10385–10388.

Basler, C.F., Wang, X., Muhlberger, E., Volchkov, V., Paragas, J., Klenk, H.D., Garcia-Sastre, A., and Palese, P. (2000). The Ebola virus VP35 protein functions as a type I IFN antagonist. Proc. Natl. Acad. Sci. U S A *97*, 12289–12294.

Basler, C.F., Mikulasova, A., Martinez-Sobrido, L., Paragas, J., Muhlberger, E., Bray, M., Klenk, H.D., Palese, P., and Garcia-Sastre, A. (2003). The Ebola virus VP35 protein inhibits activation of interferon regulatory factor 3. J. Virol. *77*, 7945–7956.

Black, B.L., and Lyles, D.S. (1992). Vesicular stomatitis virus matrix protein inhibits host cell-directed transcription of target genes in vivo. J. Virol. *66*, 4058–4064.

Cardenas, W.B., Loo, Y.M., Gale, M., Jr., Hartman, A.L., Kimberlin, C.R., Martinez-Sobrido, L., Saphire, E.O., and Basler, C.F. (2006). Ebola virus VP35 protein binds double-stranded RNA and inhibits alpha/beta interferon production induced by RIG-I signaling. J. Virol. *80*, 5168–5178.

Claude, K.M., Underschultz, J., and Hawkes, M.T. (2018). Ebola virus epidemic in war-torn eastern DR Congo. Lancet *392*, 1399–1401.

Clavarino, G., Claudio, N., Couderc, T., Dalet, A., Judith, D., Camosseto, V., Schmidt, E.K., Wenger, T., Lecuit, M., Gatti, E., et al. (2012a). Induction of GADD34 is necessary for dsRNA-dependent interferon-beta production and participates in the control of Chikungunya virus infection. PLoS Pathog. *8*, e1002708.

Clavarino, G., Claudio, N., Dalet, A., Terawaki, S., Couderc, T., Chasson, L., Ceppi, M., Schmidt, E.K., Wenger, T., Lecuit, M., et al. (2012b). Protein phosphatase 1 subunit Ppp1r15a/GADD34 regulates cytokine production in polyinosinic:polycytidylic acid-stimulated dendritic cells. Proc. Natl. Acad. Sci. U S A *109*, 3006–3011.

Connor, J.H., and Lyles, D.S. (2002). Vesicular stomatitis virus infection alters the eIF4F translation initiation complex and causes dephosphorylation of the eIF4E binding protein 4E-BP1. J. Virol. *76*, 10177–10187.

Connor, J.H., and Lyles, D.S. (2005). Inhibition of host and viral translation during vesicular stomatitis virus infection. eIF2 is responsible for the inhibition of viral but not host translation. J. Biol. Chem. *280*, 13512–13519.

Cureton, D.K., Burdeinick-Kerr, R., and Whelan, S.P. (2012). Genetic inactivation of COPI

coatomer separately inhibits vesicular stomatitis virus entry and gene expression. J. Virol. *86*, 655–666.

Dalet, A., Arguello, R.J., Combes, A., Spinelli, L., Jaeger, S., Fallet, M., Vu Manh, T.P., Mendes, A., Perego, J., Reverendo, M., et al. (2017). Protein synthesis inhibition and GADD34 control IFN-beta heterogeneous expression in response to dsRNA. EMBO J. *36*, 761–782.

Deen, G.F., Broutet, N., Xu, W., Knust, B., Sesay, F.R., McDonald, S.L.R., Ervin, E., Marrinan, J.E., Gaillard, P., Habib, N., et al. (2017). Ebola RNA persistence in semen of ebola virus disease survivors - final report. N. Engl. J. Med. *377*, 1428–1437.

Doumbo, O., Rossignol, J.F., Pichard, E., Traore, H.A., Dembele, T.M., Diakite, M., Traore, F., and Diallo, D.A. (1997). Nitazoxanide in the treatment of cryptosporidial diarrhea and other intestinal parasitic infections associated with acquired immunodeficiency syndrome in tropical Africa. Am. J. Trop. Med. Hyg. *56*, 637–639.

Elazar, M., Liu, M., McKenna, S.A., Liu, P., Gehrig, E.A., Puglisi, J.D., Rossignol, J.F., and Glenn, J.S. (2009). The anti-hepatitis C agent nitazoxanide induces phosphorylation of eukaryotic initiation factor 2alpha via protein kinase activated by double-stranded RNA activation. Gastroenterology *137*, 1827–1835.

Elion, D.L., and Cook, R.S. (2018). Harnessing RIG-I and intrinsic immunity in the tumor microenvironment for therapeutic cancer treatment. Oncotarget *9*, 29007–29017.

Feng, Z., Cerveny, M., Yan, Z., and He, B. (2007). The VP35 protein of Ebola virus inhibits the antiviral effect mediated by double-stranded RNA-dependent protein kinase PKR. J. Virol. *81*, 182–192.

Ferran, M.C., and Lucas-Lenard, J.M. (1997). The vesicular stomatitis virus matrix protein inhibits transcription from the human beta interferon promoter. J. Virol. *71*, 371–377.

La Frazia, S., Ciucci, A., Arnoldi, F., Coira, M., Gianferretti, P., Angelini, M., Belardo, G., Burrone, O.R., Rossignol, J.F., and Santoro, M.G. (2013). Thiazolides, a new class of antiviral agents effective against rotavirus infection, target viral morphogenesis, inhibiting viroplasm formation. J. Virol. *87*, 11096–11106.

Garcia-Sastre, A. (2017). Ten strategies of interferon evasion by viruses. Cell Host Microbe *22*, 176–184.

Gekonge, B., Bardin, M.C., and Montaner, L.J. (2015). Short communication: nitazoxanide inhibits HIV viral replication in monocyte-derived macrophages. AIDS Res. Hum. Retroviruses *31*, 237–241.

Haffizulla, J., Hartman, A., Hoppers, M., Resnick, H., Samudrala, S., Ginocchio, C., Bardin, M., and Rossignol, J.F.; U.S.N.I.C.S. Group (2014). Effect of nitazoxanide in adults and adolescents with acute uncomplicated influenza: a double-blind, randomised, placebo-controlled, phase 2b/3 trial. Lancet Infect. Dis. *14*, 609–618.

Hartman, A.L., Bird, B.H., Towner, J.S., Antoniadou, Z.A., Zaki, S.R., and Nichol, S.T. (2008). Inhibition of IRF-3 activation by VP35 is critical for the high level of virulence of ebola virus. J. Virol. *82*, 2699–2704.

Huang, I.C., Bailey, C.C., Weyer, J.L., Radoshitzky, S.R., Becker, M.M., Chiang, J.J., Brass, A.L., Ahmed, A.A., Chi, X., Dong, L., et al. (2011). Distinct patterns of IFITM-mediated restriction of filoviruses, SARS coronavirus, and influenza A virus. PLoS Pathog. *7*, e1001258.

Hussar, D.A. (2004). New drugs of 2003. J. Am. Pharm. Assoc. (2003) *44*, 168–206, quiz 207–210.

Kato, H., Takeuchi, O., Sato, S., Yoneyama, M., Yamamoto, M., Matsui, K., Uematsu, S., Jung, A., Kawai, T., Ishii, K.J., et al. (2006). Differential roles of MDA5 and RIG-I helicases in the recognition of RNA viruses. Nature *441*, 101–105.

Kato, H., Takeuchi, O., Mikamo-Satoh, E., Hirai, R., Kawai, T., Matsushita, K., Hiiragi, A., Dermody, T.S., Fujita, T., and Akira, S. (2008). Length-dependent recognition of double-stranded ribonucleic acids by retinoic acid-inducible gene-I and melanoma differentiation-associated gene 5. J. Exp. Med. *205*, 1601–1610.

Kawai, T., Takahashi, K., Sato, S., Coban, C., Kumar, H., Kato, H., Ishii, K.J., Takeuchi, O., and Akira, S. (2005). IPS-1, an adaptor triggering RIG-I- and Mda5-mediated type I interferon induction. Nat. Immunol. *6*, 981–988.

von Kobbe, C., van Deursen, J.M., Rodrigues, J.P., Sitterlin, D., Bachi, A., Wu, X., Wilm, M., Carmo-Fonseca, M., and Izaurralde, E. (2000). Vesicular stomatitis virus matrix protein inhibits host cell gene expression by targeting the nucleoporin Nup98. Mol. Cell *6*, 1243–1252.

Leung, D.W., Prins, K.C., Borek, D.M., Farahbakhsh, M., Tufariello, J.M., Ramanan, P., Nix, J.C., Helgeson, L.A., Otwinowski, Z., Honzatko, R.B., et al. (2010). Structural basis for dsRNA recognition and interferon antagonism by Ebola VP35. Nat. Struct. Mol. Biol. *17*, 165–172.

Li, Z., Brecher, M., Deng, Y.Q., Zhang, J., Sakamuru, S., Liu, B., Huang, R., Koetzner, C.A., Allen, C.A., Jones, S.A., et al. (2017). Existing drugs as broad-spectrum and potent inhibitors for Zika virus by targeting NS2B-NS3 interaction. Cell Res. *27*, 1046–1064.

Lin, R., Heylbroeck, C., Pitha, P.M., and Hiscott, J. (1998). Virus-dependent phosphorylation of the IRF-3 transcription factor regulates nuclear translocation, transactivation potential, and proteasome-mediated degradation. Mol. Cell. Biol. *18*, 2986–2996.

Luthra, P., Ramanan, P., Mire, C.E., Weisend, C., Tsuda, Y., Yen, B., Liu, G., Leung, D.W., Geisbert, T.W., Ebihara, H., et al. (2013). Mutual antagonism between the Ebola virus VP35 protein and the RIG-I activator PACT determines infection outcome. Cell Host Microbe *14*, 74–84.

Ma, Y., and Hendershot, L.M. (2003). Delineation of a negative feedback regulatory loop that controls protein translation during endoplasmic reticulum stress. J. Biol. Chem. *278*, 34864–34873.

Machitani, M., Sakurai, F., Wakabayashi, K., Takayama, K., Tachibana, M., and Mizuguchi, H. (2017). Type I interferons impede short hairpin RNA-mediated RNAi via inhibition of dicer-mediated processing to small interfering RNA. Mol. Ther. Nucleic Acids *6*, 173–182.

Meylan, E., Curran, J., Hofmann, K., Moradpour, D., Binder, M., Bartenschlager, R., and Tschopp, J. (2005). Cardif is an adaptor protein in the RIG-I antiviral pathway and is targeted by hepatitis C virus. Nature *437*, 1167–1172.

Minami, K., Tambe, Y., Watanabe, R., Isono, T., Haneda, M., Isobe, K., Kobayashi, T., Hino, O., Okabe, H., Chano, T., et al. (2007). Suppression of viral replication by stress-inducible GADD34 protein via the mammalian serine/threonine protein kinase mTOR pathway. J. Virol. *81*, 11106–11115.

Novoa, I., Zeng, H., Harding, H.P., and Ron, D. (2001). Feedback inhibition of the unfolded protein response by GADD34-mediated dephosphorylation of eIF2alpha. J. Cell Biol. *153*, 1011–1022.

Peisley, A., Wu, B., Yao, H., Walz, T., and Hur, S. (2013). RIG-I forms signaling-competent filaments in an ATP-dependent, ubiquitin-independent manner. Mol. Cell *51*, 573–583.

Petersen, T., Lee, Y.J., Osinusi, A., Amorosa, V.K., Wang, C., Kang, M., Matining, R., Zhang, X., Dou, D., Umbleja, T., et al. (2016). Interferon stimulated gene expression in HIV/HCV coinfected patients treated with nitazoxanide/peginterferon-Alfa-2a and ribavirin. AIDS Res. Hum. Retroviruses *32*, 660–667.

Piacentini, S., La Frazia, S., Riccio, A., Pedersen, J.Z., Topai, A., Nicolotti, O., Rossignol, J.F., and Santoro, M.G. (2018). Nitazoxanide inhibits paramyxovirus replication by targeting the Fusion protein folding: role of glycoprotein-specific thiol oxidoreductase ERp57. Sci. Rep. *8*, 10425.

Prins, K.C., Cardenas, W.B., and Basler, C.F. (2009). Ebola virus protein VP35 impairs the function of interferon regulatory factor-activating kinases IKKepsilon and TBK-1. J. Virol. *83*, 3069–3077.

Prins, K.C., Delpeut, S., Leung, D.W., Reynard, O., Volchkova, V.A., Reid, S.P., Ramanan, P., Cardenas, W.B., Amarasinghe, G.K., Volchkov, V.E., et al. (2010). Mutations abrogating VP35 interaction with double-stranded RNA render Ebola virus avirulent in Guinea pigs. J. Virol. *84*, 3004–3015.

Romark, L.C. (2017). ALINIA (Nitazoxanide): Full Prescribing Information. https://www.alinia.com/wp-content/uploads/2017/08/prescribing-information.pdf.

Rossignol, J.F. (2014). Nitazoxanide: a first-in-class broad-spectrum antiviral agent. Antivir. Res. *110*, 94–103.

Rossignol, J.F., and El-Gohary, Y.M. (2006). Nitazoxanide in the treatment of viral gastroenteritis: a randomized double-blind placebo-controlled clinical trial. Aliment. Pharmacol. Ther. *24*, 1423–1430.

Rossignol, J.F., Hidalgo, H., Feregrino, M., Higuera, F., Gomez, W.H., Romero, J.L., Padierna, J., Geyne, A., and Ayers, M.S. (1998). A double-'blind' placebo-controlled study of nitazoxanide in the treatment of cryptosporidial diarrhoea in AIDS patients in Mexico. Trans. R. Soc. Trop. Med. Hyg. *92*, 663–666.

Rossignol, J.F., Abu-Zekry, M., Hussein, A., and Santoro, M.G. (2006). Effect of nitazoxanide for

treatment of severe rotavirus diarrhoea: randomised double-blind placebo-controlled trial. Lancet *368*, 124–129.

Rossignol, J.F., Kabil, S.M., El-Gohary, Y., Elfert, A., and Keeffe, E.B. (2008). Clinical trial: randomized, double-blind, placebo-controlled study of nitazoxanide monotherapy for the treatment of patients with chronic hepatitis C genotype 4. Aliment. Pharmacol. Ther. *28*, 574–580.

Rossignol, J.F., Elfert, A., El-Gohary, Y., and Keeffe, E.B. (2009a). Improved virologic response in chronic hepatitis C genotype 4 treated with nitazoxanide, peginterferon, and ribavirin. Gastroenterology *136*, 856–862.

Rossignol, J.F., La Frazia, S., Chiappa, L., Ciucci, A., and Santoro, M.G. (2009b). Thiazolides, a new class of anti-influenza molecules targeting viral hemagglutinin at the post-translational level. J. Biol. Chem. *284*, 29798–29808.

Schlee, M., Roth, A., Hornung, V., Hagmann, C.A., Wimmenauer, V., Barchet, W., Coch, C., Janke, M., Mihailovic, A., Wardle, G., et al. (2009). Recognition of 5′ triphosphate by RIG-I helicase requires short blunt double-stranded RNA as contained in panhandle of negative-strand virus. Immunity *31*, 25–34.

Schumann, M., Gantke, T., and Muhlberger, E. (2009). Ebola virus VP35 antagonizes PKR activity through its C-terminal interferon inhibitory domain. J. Virol. *83*, 8993–8997.

Sekiba, K., Otsuka, M., Ohno, M., Yamagami, M., Kishikawa, T., Suzuki, T., Ishibashi, R., Seimiya, T., Tanaka, E., and Koike, K. (2018). Inhibition of HBV transcription from cccDNA with nitazoxanide by targeting the HBx-DDB1 interaction. Cell Mol. Gastroenterol. Hepatol. *7*, 297–312.

Seth, R.B., Sun, L., Ea, C.K., and Chen, Z.J. (2005). Identification and characterization of MAVS, a mitochondrial antiviral signaling protein that activates NF-kappaB and IRF 3. Cell *122*, 669–682.

Shiwani, H.A., Pharithi, R.B., Khan, B., Egom, C.B., Kruzliak, P., Maher, V., and Egom, E.E. (2017). An update on the 2014 Ebola outbreak in Western Africa. Asian Pac. J. Trop. Med. *10*, 6–10.

Staeheli, P., and Pavlovic, J. (1991). Inhibition of vesicular stomatitis virus mRNA synthesis by human MxA protein. J. Virol. *65*, 4498–4501.

Trabattoni, D., Gnudi, F., Ibba, S.V., Saulle, I., Agostini, S., Masetti, M., Biasin, M., Rossignol, J.F., and Clerici, M. (2016). Thiazolides elicit anti-viral innate immunity and reduce HIV replication. Sci. Rep. *6*, 27148.

Unterholzner, L., and Almine, J.F. (2019). Camouflage and interception: how pathogens evade detection by intracellular nucleic acid sensors. Immunology *156*, 217–227.

Weidner, J.M., Jiang, D., Pan, X.B., Chang, J., Block, T.M., and Guo, J.T. (2010). Interferon-induced cell membrane proteins, IFITM3 and tetherin, inhibit vesicular stomatitis virus infection via distinct mechanisms. J. Virol. *84*, 12646–12657.

World Health Organization (2019). https://www.who.int/ebola/situation-reports/drc-2018/en/.

Xu, L.G., Wang, Y.Y., Han, K.J., Li, L.Y., Zhai, Z., and Shu, H.B. (2005). VISA is an adapter protein required for virus-triggered IFN-beta signaling. Mol. Cell *19*, 727–740.

Yong, H.Y., and Luo, D. (2018). RIG-I-like receptors as novel targets for pan-antivirals and vaccine adjuvants against emerging and re-emerging viral infections. Front. Immunol. *9*, 1379.

ISCI, Volume *19*

Supplemental Information

The FDA-Approved Oral Drug Nitazoxanide Amplifies Host Antiviral Responses and Inhibits Ebola Virus

Luke D. Jasenosky, Cristhian Cadena, Chad E. Mire, Viktoriya Borisevich, Viraga Haridas, Shahin Ranjbar, Aya Nambu, Sina Bavari, Veronica Soloveva, Supriya Sadukhan, Gail H. Cassell, Thomas W. Geisbert, Sun Hur, and Anne E. Goldfeld

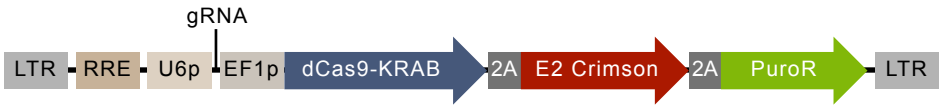

A Human PKR gene promoter

5'…TGGGGGCCAAGCCCGCCGGTGCCAAGCCCGCCCGCCAGTGCCTCTCGCGCGCACTCTGG

ATCCAGCGCCAATTTACCCCAATCCCGTAGCAGACGAGGGCTTGTGCGAGAGGGGGCCGGG

gRNA ISRE

CGGCTGCAGGGAAGGCGGAGTCCAAGGGGAAAACGAAACTGAGAACCAGCTCTCCCGAAGC

guide RNA

CGCGGGTCTCCGGCCGGCGGCGCGGCGGCGGCGGCGGCGGCGCAGGTGAGCAGGG…3'

+1

B Human RIG-I gene promoter

5'…CCGGGCTTCCTCGGTGCGGAGGGAAACGAAACTAGCCCGAGGCAAAACAGCCTCCGC

IRF1 binding site

GAACCCCGCCCGCCGCTAGTTGCACTTTCGATTTTCCCTTTAGTTATTAAAGTTCCTAT

guide RNA +1

GCAGCTCCGCCTCGCGTCCGGCCTCATTTCCTCGGAAAATCCCTGCTTTCCCCGCTCGC

CACGCCCTCCTCCTACCCGGCTTTAAAGCTAGTGAGGCACAGCCTGCGGGGAACGTAGC

TAGCTGCAAGCAGAGGCCGGCATG…3'

C Human GADD34 gene promoter

5'…TGAGAGAGAACTGGCTCGCTGTTGAAGCAGGGCCACGCATTTGATTGACAGTTCGTT

TGTTGGAGGGGCGTGGTCACGCTCGGAAACTCCGCCGTGACGTTGCAAAAGCTGGAATC

TCCGCGAGAAGTCCTGTCTTACTTCCACTTCCCACCCTTCGGGTTGCGGTCTCGAAACC

ATF4 site TATA box

CCGCCTCTCTTCGTGACGTCAGCACGCCGGGCGCGGTAGGCTATAAAAGCCTAGTGGCC

guide RNA

ATTGTGTTCGTTGCTCTTATCGGTTCCCATCCCAGTTGT…3'

+1

Legend Supplementary Figure 1. Promoter sequences targeted for CRISPR/dCas9-KRAB-mediated gene knockdown, related to Figure 3. Sites targeted in the promoters of A) PKR, B) RIG-I, and C) GADD34 with specific guide RNAs to suppress transcription with dCas9-KRAB.

Transparent Methods

IFN-β promoter reporter assay

For RNA-mediated stimulation of the RLR pathway, HEK 293Ts were maintained in 48-well plates in Dulbecco's modified Eagle medium (Cellgro) supplemented with 10% heat-inactivated fetal calf serum (FBS). The next day, cells were transfected with 10 ng of pFLAG-CMV4 plasmid encoding RIG-I, MDA5, or an empty vector control (Ahmad et al., 2018; Wu et al., 2014), together with 100 ng of IFNβ promoter-driven firefly luciferase reporter plasmid and 10 ng of CMV promoter-driven Renilla luciferase reporter plasmid (Lipofectamine2000, Life Technologies). The medium was changed 4 hours post-transfection with DMEM containing 1% FBS and the indicated concentration of NTZ. All experiments involving NTZ were performed in this manner in order to reduce the impact of serum proteins on NTZ's function in tissue culture, as NTZ is highly protein-bound (Stockis et al., 1996). Four hours after addition of NTZ (Sigma), cells were transfected with 200ng of high molecular weight poly I:C (Invivogen), *in vitro* transcribed 42bp dsRNA (1AB) (sequence: gggaga atgtcgaatgggtattccacagacgagaatttccgctatctctccc), or mock transfected with water. For stimulation of downstream IFN signaling components, HEK 293Ts were transfected with 10 ng of pFLAG-CMV4 encoding MDA5 or MAVS (Wu et al., 2014), the indicated amount of the phosphomimetic IRF3-5D (Mutations Ser^{396}, Ser^{398}, Ser^{402}, Thr^{404}, and Ser^{405} to Glu) or empty vector. The medium was changed 4 hours post-transfection with DMEM containing 1% FBS and the indicated concentration of NTZ. Cells were lysed ~20 hr post-stimulation and IFN promoter activity was measured using the Dual

Luciferase Reporter assay (Promega) and a Synergy2 plate reader (BioTek). Firefly luciferase activity was normalized against Renilla luciferase activity.

qPCR

To measure endogenous IFN-β mRNA levels upon 1AB stimulation, HEK 293T cells in 48-well plates were pre-treated with the indicated concentration of NTZ in DMEM containing 1% FBS. Four hours after addition of NTZ, cells were transfected with 200 ng of 1AB. RNA was extracted 20 hours after stimulation using Tri Reagent and Direct-zol RNA miniprep (Zymo Research). cDNA was prepared using the High-capacity RT kit (Applied Biosystems) with random primers, and qPCR was done using Power SYBR Green PCR Master Mix (Applied Biosystems). For paracrine stimulation of the IFN pathway, HEK 293T cells were maintained in DMEM supplemented with 10% FBS. As described above, the next day the medium was changed with DMEM containing 1% FBS and the indicated concentration of NTZ for 4 hrs, followed by stimulation with 10 ng/mL recombinant human IFN-β (PeproTech),. Cells were harvested ~20 hr post-stimulation and qPCR was performed as described above. CT values were normalized to Glyceraldehyde 3-phosphate dehydrogenase (GAPDH). Relative quantification was calculated by the comparative CT method and is shown as fold change of expression ($2^{-\Delta\Delta CT}$).

To test if NTZ induces GADD34 gene expression, A549 cells grown in 10% FBS/DMEM were switched to 1% FBS/DMEM for 1 hour and then treated with 0, 10, 20, or 30 μM NTZ for 4 hours, followed by RNA isolation and oligoDT-based cDNA

synthesis. CT values were normalized to cyclophilin A as a housekeeping gene and relative quantitation of GADD34 mRNA levels was performed as described above.

Effect of NTZ on VSV-Luc replication in A549 cells

A549 cells were maintained as described above and treated with vehicle or increasing concentrations of NTZ up to 30 μM for 4 hrs. Next, cells were infected with VSV-Luc (a gift from Martin Dorf) and 16 hrs post-infection cells were lysed and firefly luciferase activity was measured as directed by the manufacturer (Biotium).

Efficacy of NTZ pre-treatment on inhibition of VSV-Luc infection was compared in the CRISPR/dCas9-KRAB control, PKR-KD, RIG-I-KD, and GADD34-KD A549 cell lines (see cell line description below) as described above for wild-type A549 cells. In all cases, equivalent numbers of each cell line were seeded one day prior to NTZ treatment and subsequent VSV-Luc infection.

CRISPR/dCas9-KRAB-based knock down of gene expression in A549 cells and effect of NTZ on VSV-Luc replication in A549 cell lines

To stably co-express dCas9-KRAB and a guide RNA specific to the promoters of the genes encoding i) PKR, ii) RIG-I, or iii) GADD34, a lentiviral vector was constructed that encoded an EFS promoter-driven dCas9-KRAB-2A-E2Crimson-2A-puroR cassette and a U6 promoter for gRNA transcription (see Supp. Fig. 1) based on similar approaches our laboratory has used previously (Chow et al., 2014). Individual gRNA sequences were obtained from the CRISPR design program at crispr.mit.edu and are shown in Supplemental Figure 1, along with the sites in the individual gene promoters that they

target. As a control, a lentiviral vector encoding a U6 promoter-driven scrambled gRNA that does not match any genomic sequence was also constructed (designated CRISPR-control).

To generate A549 cells with stable knock down of specific genes, cells were transduced with the control or gene-specific lentiviruses, and positively transduced cells were selected with 2 μg/ml puromycin for 3 weeks as described previously (Chow et al., 2014). Efficacy of the knockdowns was then evaluated by analyzing gene expression following mock stimulation or stimulation with 100 ng/ml human IFN-β for 4 hours for the CRISPR-control, CRISPR-RIG-I, and CRISPR-PKR cells, or with 40 μM NTZ for 8 hours for the CRISPR-control and CRISPR-GADD34 cells. RNA was isolated and reverse transcribed using anchored oligoDT priming and cDNA was measured using standard qPCR methodology and normalized to the housekeeping gene cyclophilin B with the primers shown in the legend of Fig. 3.

Western Blot Analysis

The CRISPR A549 cell lines were cultured in DMEM/F12 complete media and used for Western blotting. For GADD34 detection, CRISPR-control and CRISPR-GADD34 cells were stimulated by tunicamycin (TN) at 10 μg/ml or NTZ at 25 μM for 8 hours then harvested and used for Western blotting. Cell pellets were lysed in Laemmli buffer (62.5 mM Tris-HCl [pH 6.8], 2% sodium dodecyl sulfate, 2.5% beta-mercaptoethanol, 10% glycerol, and 0.01% bromophenol blue; BIO-RAD) for 30 min in presence of protease inhibitors (Thermo Fisher Scientific), boiled for 5 min at 100ºC, and subjected to Western blot analysis. Primary antibodies: DDX58 (RIG-I) (1:2,000,

D14G6, 3743, Cell Signaling Technology), EIF2AK2 (PKR) (1:5,000, Y117, ab32506, abcam), PPP1R15A (GADD34) (1:10000, polyclonal, 10449-1-AP, Proteintech) and TUBA4A (alpha-Tublin) (1: 5,000, B-5-1-2, T5168, SIGMA). Blots were probed with anti-mouse (1:2,000, 7076, Cell Signaling Technology) or anti-rabbit (1:2,000, 7074, Cell Signaling Technology) IgG-HRP secondary antibody and visualized using SuperSignal West Pico PLUS Chemiluminescent Substrate (Thermo Fisher Scientific) or SuperSignal West Femto Maximum Sensitivity Substrate (Thermo Fisher Scientific).

NTZ inhibition of live EBOV infection in A549 cells and CRISPR/dCas9-KRAB-based knock down of gene expression in A549 cells

To assess the ability of NTZ treatment to inhibit replication of authentic EBOV in A549 cells, we infected cells in duplicate with the *Zaire ebolavirus* Kikwit strain (EBOV). After 1 hour in DMEM+1%FBS cells were treated with 20 μM or 40 μM NTZ for 4 hours before EBOV infection. After the 4-hour pre-treatment, the supernatants from the NTZ-treated cells were removed and then used to make up the EBOV inocula per condition. Cells were inoculated at an MOI of 0.01, which was rocked at 37°C for one hour. The inocula were left on the cells and had fresh media containing 20 μM or 40 μM NTZ added. Supernatants were collected at 1, 48, and 72 hours post infection and analyzed for production of infectious virus by plaque assay analysis.

The A549 cells with CRISPR/dCas9-KRAB-based knock down of: i) PKR, ii) RIG-I, or iii) GADD34 were used to assess the mechanism of NTZ EBOV inhibition through these genes. For this analysis, we infected cells in duplicate with the *Zaire ebolavirus* Kikwit strain (EBOV). After 1 hour in DMEM+1%FBS cells were treated

with 20 μM NTZ for 4 hours before EBOV infection. After the 4-hour pre-treatment, the supernatants from the NTZ-treated cells were removed and then used to make up the EBOV inocula per condition. Cells were inoculated at an MOI of 0.01, which was rocked at 37°C for one hour. The inocula were left on the cells and had fresh media containing 20 μM NTZ added. Supernatants were collected at 1, 48, and 72 hours post infection and analyzed for production of infectious virus by plaque assay analysis.

Virus titration was performed on Vero E6 cells from all supernatants collected. Increasing ten-fold dilutions of each sample were adsorbed to the cell monolayers in duplicate wells (200 μl each); the limit of detection of the assay was 25 plaque forming units per milliliter.

References for Transparent Methods

Ahmad, S., Mu, X., Yang, F., Greenwald, E., Park, J.W., Jacob, E., Zhang, C.Z., and Hur, S. (2018). Breaching Self-Tolerance to Alu Duplex RNA Underlies MDA5-Mediated Inflammation. Cell *172*, 797-810 e713.

Chow, N.A., Jasenosky, L.D., and Goldfeld, A.E. (2014). A distal locus element mediates IFN-gamma priming of lipopolysaccharide-stimulated TNF gene expression. Cell Rep *9*, 1718-1728.

Li, S., Wang, L., Berman, M., Kong, Y.Y., and Dorf, M.E. (2011). Mapping a dynamic innate immunity protein interaction network regulating type I interferon production. Immunity *35*, 426-440.

Stockis, A., Deroubaix, X., Lins, R., Jeanbaptiste, B., Calderon, P., and Rossignol, J.F. (1996). Pharmacokinetics of nitazoxanide after single oral dose administration in 6 healthy volunteers. Int J Clin Pharmacol Ther *34*, 349-351.

Wu, B., Peisley, A., Tetrault, D., Li, Z., Egelman, E.H., Magor, K.E., Walz, T., Penczek, P.A., and Hur, S. (2014). Molecular imprinting as a signal-activation mechanism of the viral RNA sensor RIG-I. Mol Cell *55*, 511-523.